

EXPERIMENTAL AND NUMERICAL ANALYSIS ON LIFT AND TRANSITION CHARACTERISTICS OF ONERA-M5 CONFIGURATION MODEL

Kenji YOSHIDA, Yoshine UEDA and Masayoshi NOGUCHI

Japan Aerospace Exploration Agency, 6-13-1, Osawa, Mitaka, Tokyo, 181-0015, Japan

Keywords: *wind tunnel test, transition measurement, e^N method, CFD, short bubble*

Abstract

The authors investigated the aerodynamic characteristics of “ONERA-M5” model experimentally and numerically. Two important subjects were considered. The first one is to obtain its boundary layer transition characteristics at transonic speed, because all transition data is very useful for aerodynamic designers to improve the aerodynamic performance of subsonic aircrafts at cruise condition. The transition characteristics on the wing and nose part of the model were measured by an IR camera technique and Preston tubes. Then they were compared with transition prediction results by an e^N method developed by JAXA, and good agreement was found under an assumed transition criterion of N value. The second subject is to understand the Reynolds number effect on the lift characteristics of the model at low speed, because a prediction of its high Reynolds number effect is strongly required for aerodynamic designers in developing a real aircraft. The Reynolds number effect on the lift characteristics of the model was obtained by both force and pressure measurements under some transition conditions. So-called “adverse Reynolds number effect” on the lift characteristics was not observed in the test Reynolds number range, because the wing had a remarkable feature of the leading-edge stall type. Therefore, the maximum lift condition was dominated by the short bubble burst. Furthermore an artificial condition of fixing the transition location on its attachment-line was confirmed to improve the lift characteristics and to show the measured pressure distributions

were very similar to the computational results by CFD with all turbulent state condition.

1 Introduction

“ONERA-M5” configuration model is well known to be one of standard configuration models which are used to investigate transonic wind tunnel performance. This model is so fundamental, but it has essential components of a subsonic transport aircraft, that is a swept tapered wing, a nose cone, a wide straight fuselage, a horizontal and vertical tails. Presently, we understand its force and pressure distributions on the surface very well through a great amount of works. However, its boundary layer transition characteristics at transonic speed are not investigated well. Transition data is very effective in researching the improvement of cruise drag performance.

In engineering field, establishment of a transition prediction method is one of the important subjects. Today, an e^N method based on stability theory of laminar boundary layer is used as the most effective technique and many research works are advanced at low, transonic [1] and supersonic speed [2]. To predict transition location using an e^N method, a certain criterion of the so-called N value is required. In obtaining such a criterion, numerous reliable transition data must be obtained experimentally. Therefore, the transition measurement tests on the wing and nose part of the ONERA-M5 model are expected to be very effective in both transition research and aerodynamic design fields.

As another subject, Reynolds number effect on aerodynamic characteristics of the ONERA-M5 configuration was also selected. In the aerodynamic design of aircrafts, the estimation of high Reynolds number effect on maximum lift from wind tunnel test results is very important. In general, the maximum lift is expected to increase with an increase in Reynolds number. However, some results on the decrease of the maximum lift were experimentally observed [3][4]. This phenomenon is called “adverse Reynolds number effect”. Its mechanism is qualitatively explained as follows [3]. In a simple swept wing, transition due to attachment-line contamination occurs near the leading-edge at high Reynolds numbers. This means that turbulent boundary layer on the upper surface grows from the stagnation point. In this situation, local maximum section lift generally decreases. The swept wing has usually local maximum section lift at about 70 to 80% semi-spanwise station. If the local maximum lift decreases, the total lift also decreases. However, the reference [3] has never given any method to predict the adverse Reynolds number effect. Therefore, any detail works are strongly desired [5][6].

Therefore, as a first step of such a trial, it is valuable to investigate the Reynolds number effect on the lift performance of the ONERA-M5 model. However, we can not obtain any data from such a viewpoint.

According to those requirements above mentioned, the authors investigated the aerodynamic characteristics of the “ONERA-M5” mode experimentally and numerically. As for the first subject, transition measurement tests were conducted at JAXA 2m×2m transonic wind tunnel on the condition of Mach number 0.7, using the IR camera technique on the wing surface and the Preston tube technique on the body surface of the nose part of the model. Then their test results were compared with the transition prediction results based on the e^N code developed by present authors [2][7] to show its effectiveness.

As for the second subject, lift and pressure measurement test were performed with the variation of stagnation pressure at Mach number

0.25 condition, which was the under limit of operating the tunnel. To understand physical mechanism of Reynolds number effect on the lift characteristics, the following three kinds of transition condition were investigated; (1) natural transition (“Clean” case), (2) fixed transition on the nose part upstream the wing-body junction (“Nose Roughness” case), and (3) fixed transition on the attachment-line along full span (“LE Roughness” case). The second and third cases were introduced to investigate the effect of attachment-line contamination based on the turbulent boundary layer on the nose surface of the model. In addition, CFD(NS) computations with all turbulent condition were compared with measured pressure distributions in order to confirm the effect of the “LE Roughness” case on the pressure distributions.

In this paper, the transition measurement and analysis results at transonic speed are summarized in section 2. In addition, the study on the Reynolds number effect on the lift characteristics at low speed is described in section 3.

2 Transition Characteristics at Transonic Speed

2.1 Transition Characteristics on Wing

Figure 1 shows a photograph of test set-up of the model in JAXA 2m×2m transonic wind tunnel and a grid pattern for JAXA’s CFD code (“UPACS” code) [8]. The ONERA-M5 has the same airfoil section with no twist angle over full span, but it has both set angle of 4 degrees and dihedral angle of 3 degrees at wing-body junction. Thus this wing has a feature of tip stall type.

Figure 2 shows the comparison of measured pressure distributions (indicated as “TWT1”) and CFD computational results (indicated “CFD”) on the upper surface of the wing at two typical spanwise stations, that is $\eta=y/s=0.285$ and 0.815 . Since this wing has strong suction peak near the leading-edge, transition measurement should be conducted below the angle of attack where laminar

separation occurred. Naturally such an angle of attack corresponds to the cruise condition. The laminar separation point, estimated by a boundary layer code [9] based on the measured pressure distributions, is also plotted in the figure.

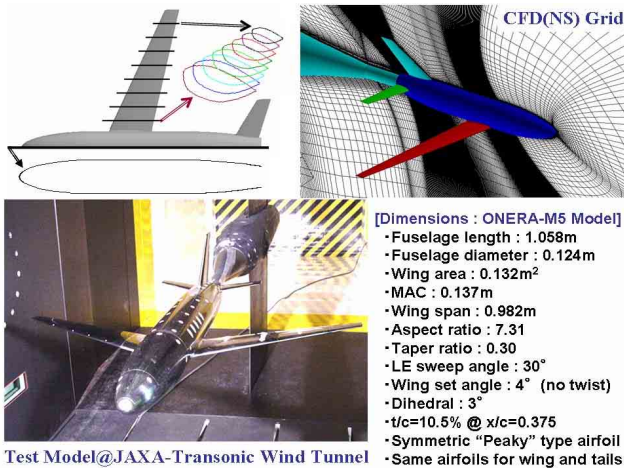


Fig. 1. ONERA-M5 wind tunnel model and CFD grid

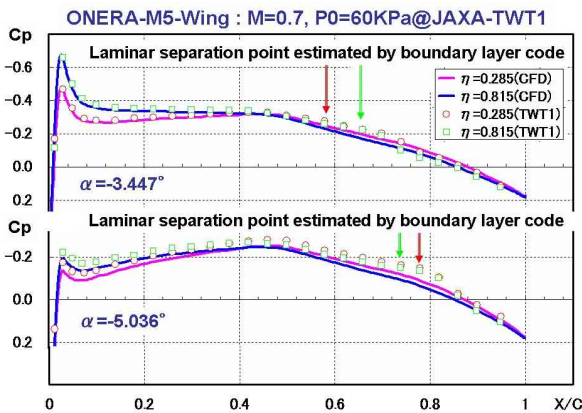


Fig. 2. Comparison of measured and estimated pressure distributions at M=0.7

In the wind tunnel test, transition was detected using the IR camera technique. In general, the IR camera technique is one of the most powerful tools to obtain the whole transition pattern on the surface. To detect its transition location clearly, a wind tunnel model should be made of adiabatic material or adiabatic coating. However, the ONERA-M5 model is made of steel. Therefore, in applying the IR camera technique to the model, we

improved the usual measurement approach by varying the stagnation temperature of the tunnel as fast as possible [10]. Furthermore, some tiny roughness was pre-set near the leading-edge to make the judgment of transition location easily by comparing with turbulent wedge from the roughness. The transition measurement was conducted at the condition of $M=0.7$ and stagnation pressure $P_0=60\text{KPa}$ and the Reynolds number based on the mean aerodynamic chord ($MAC=0.137\text{m}$) was $Rec=1.05$ million. The transition measurement results on three angles of attack are summarized in Figure 3.

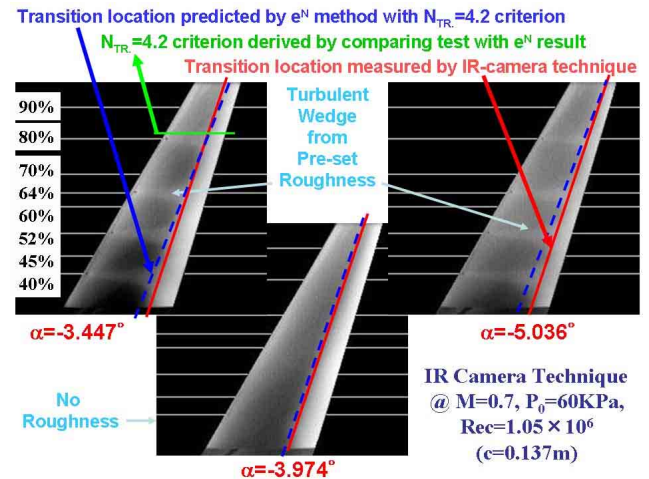


Fig. 3. Comparison of measured and predicted transition locations at M=0.7

Transition characteristics were also analyzed using our e^N code [2][7]. In this analysis, one assumption for specifying a threshold of N value as a transition criterion was required. Comparing the detected transition location with an envelope of estimated N growth at a typical spanwise station ($y/s=0.815$), the transition criterion of $N_{TR}=4.2$ was derived. Naturally this value strongly depends on freestream turbulence in the wind tunnel. Therefore, it must be determined by a comparison of measured transition and estimated N value in a typical test condition. However, if we apply this transition criterion, each transition location along the span at each angle of attack are numerically predicted as shown in Figure 3. In the figure, we obtained almost good agreement between them. It means

present e^N method works well to predict transition location under the only assumption for the transition criterion of N value. Furthermore, since the ONERA-M5 has strong adverse pressure gradient near the leading-edge and gradual adverse pressure gradient after the mid-chord at small lift condition ($\alpha=-4^\circ$), natural transition predicted by the e^N method generally occurs extremely near the laminar separation point.

2.2 Transition Characteristics on Nose

In order to improve aerodynamic performance at cruise condition, laminarization over the nose region of a subsonic aircraft is one of the most effective concepts. In general, since the nose geometry is nearly axisymmetric, its transition characteristics are simple at zero angle of attack condition. However, such geometry induces a complex flowfield with strong three-dimensionality at nonzero angle of attack condition. Therefore, its transition characteristics are supposed to become complex. To obtain such transition characteristics and to understand its behavior with variation of angle of attack, transition measurement and numerical analysis on the ONERA-M5 model were conducted.

Since the nose part of the model consists of not-so-thin material, the improved IR camera technique above mentioned was not applied to present transition measurement test. Therefore, we used a Preston tube technique which was well-known as a traditional and simple technique. In the transition measurement test with the Preston tube, some flow conditions must be varied during the operation. For example, stagnation pressure P_0 or angle of attack α should be varied.

First of all, at zero angle of attack condition, P_0 -sweep test was conducted with three Preston tubes fixed on each location, which was indicated by streamwise location $X(\text{mm})$ and circumference direction angle $\Phi(^\circ)$. Figure 4 shows the test result. Here Φ_p indicates the circumference direction angle of Preston tubes. In general, measured total pressure in a Preston tube varies rapidly from low to high

value at transition region. Therefore, we can approximately define the onset and end of transition at each streamwise location of the Preston tube as demonstrated in the figure. Exactly speaking, we found a remarkable inconsistency between the test results at $\Phi_p=90^\circ$ and $\Phi_p=-90^\circ$ cases. We consider that it originates in a little lack of symmetric feature of incoming flow or model set-up condition. Therefore, present consideration is limited to the $\Phi_p=90^\circ$ condition only.

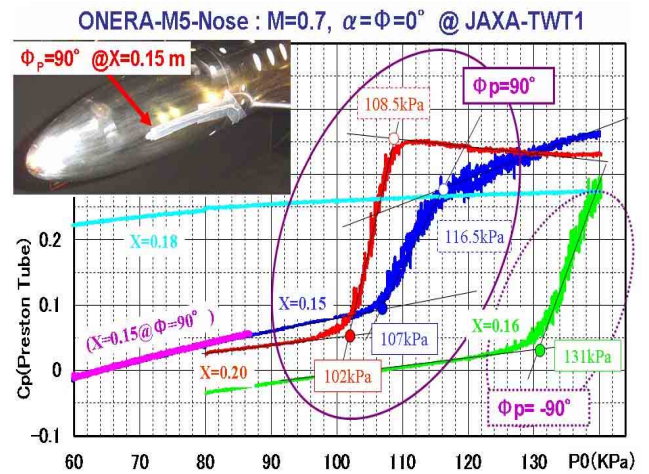


Fig. 4. Measured pressure of Preston tube on the nose surface at $M=0.7$

Transition analysis also was conducted and summarized in Figure 5. Comparing the P_0 -sweep test results with estimated N values, the transition criteria for the onset and end of

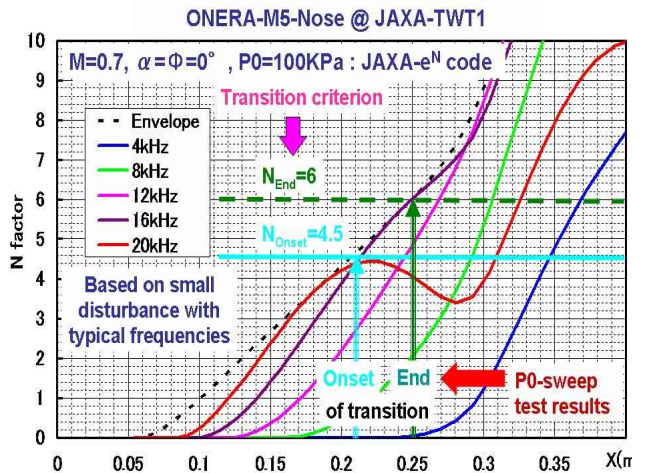


Fig. 5. Predicted envelope of each N value by e^N method and estimation of transition criteria at $M=0.7$

transition were derived as $N_{\text{onset}}=4.5$ and $N_{\text{end}}=6$ respectively.

Then, the non-axisymmetrical transition characteristics were measured in the α -sweep test or the role angle Φ -sweep test. For limitation of blow time, transition data enough to compose whole transition location pattern were not obtained. Therefore, we paid our attention to understand the whole transition pattern in comparing the test results with transition analysis results.

However, in analyzing transition characteristics on such three dimensional boundary layer at nonzero angle of attack condition, it is not easy to treat with usual boundary layer code. Present authors have already developed a new transition analysis system for such a flowfield, but at supersonic speed condition [2]. Then we applied it to analyze present transition characteristics. Figure 6 shows the results of three dimensional laminar boundary layer velocity profiles computed by JAXA's CFD(NS) code [8]. This computation was conducted at the condition of $M=0.7$, $\alpha=2^\circ$ and $P_0=100\text{KPa}$ ($\text{Reu}=12.8$ million[1/m]). Using the boundary layer data, each N value distribution was predicted as shown in Figure 7.

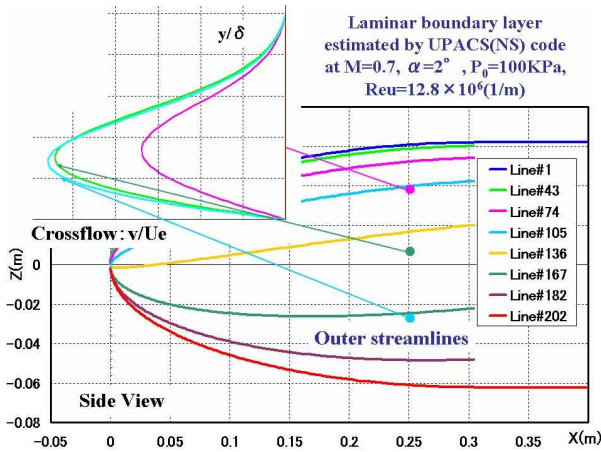


Fig. 6. Computed three dimensional laminar boundary layer velocity profiles and some streamlines at $M=0.7$ and $\alpha=2^\circ$

According to the estimation of $X=0.21\text{m}$ for the onset of transition location, the transition criterion of N value was assumed to be $N=4.5$. It

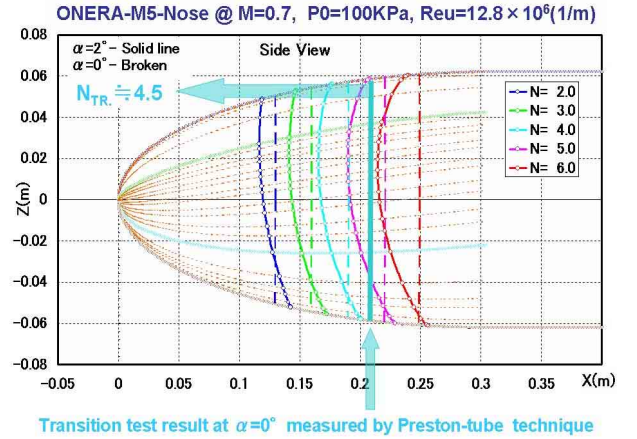


Fig. 7. Transition prediction result on the nose cone at $M=0.7$ and $\alpha=2^\circ$

is reasonable that it is nearly equal to the previous mentioned transition criterion of $N=4.2$ obtained in the transition measurement test on the wing in the same tunnel. If this criterion is applied, we can easily predict transition characteristics on the nose surface at nonzero angle of attack condition.

From present prediction result, the transition characteristics were not so complex. They were rather very simple. Therefore, we supposed transition pattern at any angle of attack condition, using the following interpolation method for the difference of the streamwise transition location between at typical angle of attack and at zero condition.

- $X_{TR} = \text{function}(\phi, \alpha, N_{TR})$
- $\Delta X_{TR}(\phi, \alpha, N_{TR}) \equiv X_{TR}(\alpha) - X_{TR}(\alpha = 0)$
- $\Delta X_{TR} = \sum_{n=0}^6 A_n(\alpha) \phi^n : \text{Polynomial approx. in } \phi$
- $A_n(\alpha) = \sum_{m=0}^2 B_m \alpha^m : \text{Polynomial approx. in } \alpha$

To improve the accuracy of such an interpolation, we selected the four transition analysis results by our e^N code with NS-based laminar boundary layer profiles at $\alpha=0, 1, 2, 3^\circ$. In addition, each expansion coefficient was estimated by least square approximation. According to present approximation, whole transition patterns on the nose surface at any

angle of attack conditions was predicted with the transition criterion of $N=4.5$ as shown in Figure 8.

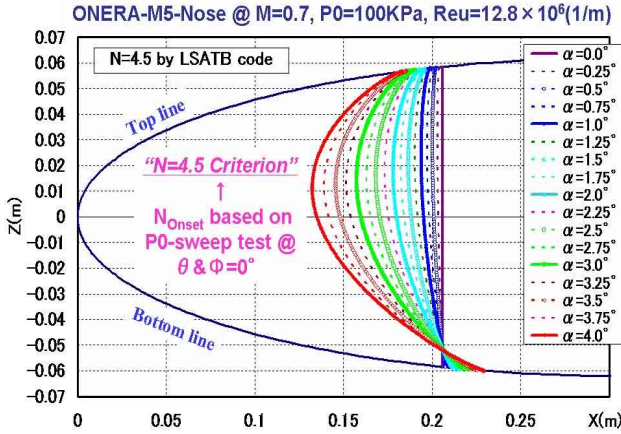


Fig. 8. Approximated transition prediction on the nose at any angle of attack condition at $M=0.7$

Finally, it was able to compare the Preston tube test results with present predictions. Figure 9 shows the transition pattern in $\Phi-\alpha$ plane. Each solid symbol corresponds to estimated onset of transition location based on the Preston tube measurements. On the other hand, each open symbol indicates predicted results at each streamwise location with the criterion of $N=4.5$.

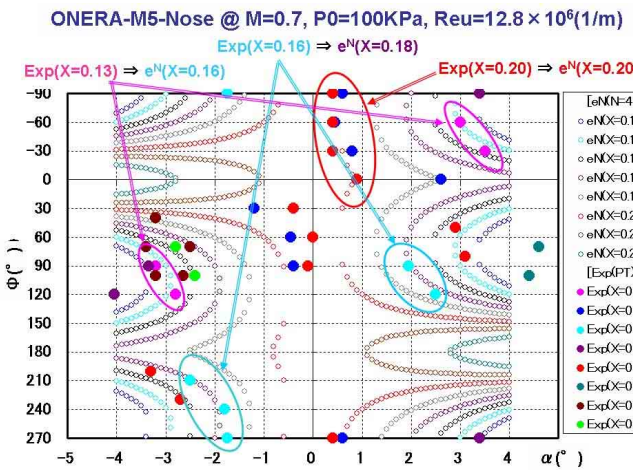


Fig. 9. Comparison of measure and predicted transition patterns on the nose cone at nonzero angle of attack conditions at $M=0.7$.

Although good agreement between the test result and predicted results was not always observed, significant correlation between them was found out in the region indicated by large

circles. Naturally the quantitative difference of transition pattern strongly depends on the criterion of the N value. Exactly speaking, although our transition prediction method is not well validated experimentally for the case of axisymmetrical body at nonzero angle of attack condition, present prediction system is supposed to be qualitatively useful, because some high correlation is found in the comparison as mentioned above. We consider that the improvement of accuracy of transition measurement on the nose surface is necessary.

3 Lift Characteristics at Low Speed

3.1 Wind Tunnel Test

The main objective of this subject is to investigate whether the ONERA-M5 model shows adverse Reynolds number effect on its lift characteristics at high Reynolds number condition or not. According to the qualitative physical explanation of the adverse Reynolds number effect described in the first section of present paper, the key point is that turbulent boundary layer extremely near the leading-edge occurs due to attachment-line contamination. Therefore, we planed the following three test conditions: (1) natural transition case (denoted as “Clean”), (2) fixed transition on the nose part upstream the wing-body junction (denoted as “Nose Roughness”), and (3) fixed transition on the leading-edge along full span (denoted as “LE Roughness”). The test set-up for each condition is demonstrated in Figure 10.

The force and pressure measurements on the wing surface were conducted. And we also measured pressure in two Preston tubes placed at $x/c=0.1$ on the right wing and in one Preston tube on the left side of the body near the wing-body junction. Present test conditions were $M=0.25$ and $P_0=70, 100, 140\text{KPa}$. The first and third ones of the P_0 are limit values on the JAXA transonic wind tunnel. $M=0.25$ is also under limit of operating the transonic wind tunnel.

Figure 10 shows the measured lift characteristics of the model at three different

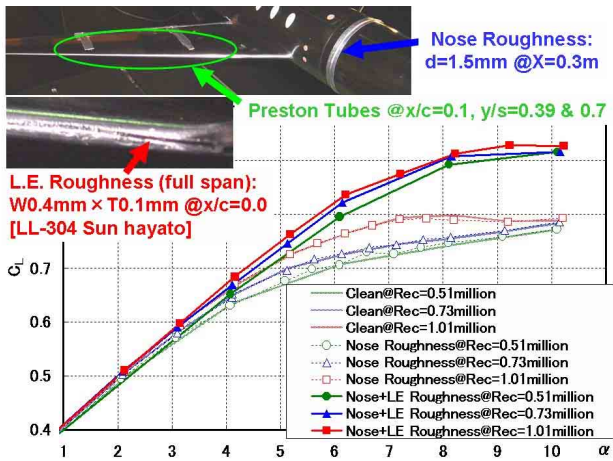


Fig. 10. Measured lift characteristics of the ONERA-M5 model at M=0.25

Reynolds number and roughness conditions. First of all, no adverse Reynolds number effect on the lift was observed in all test cases. And there was little difference of lift curves between at the “Clean” and “Nose Roughness” conditions. This means that the boundary layer on the body surface near the wing-body junction is turbulent even at the “Clean” condition. This is also indicated in Figure 11. This figure shows the pressure coefficient of the Preston tube placed on the left side of the body near the wing-body junction with variation in the angle of attack. All Cp value corresponds to turbulent state except one case of low Reynolds number condition.

Against our expectation, remarkable

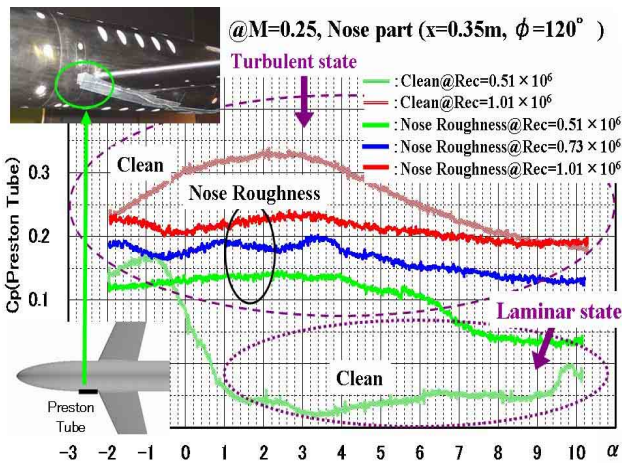


Fig. 11. Measured pressure of Preston tube on the body surface near the wing-body junction at M=0.25

increases on the lift characteristics due to the “Nose+LE Roughness” effect were also observed in Figure 10. This means turbulent boundary layer near the leading-edge does not always generate any decrease of section lift related to reducing total lift. However, we should remember that this is based on the following facts: (1) this test was conducted at relatively low Reynolds number range, (2) a possibility of relaminarization has not been denied yet.

To investigate such fact in detail, we considered measured pressure distributions as shown in Figures 12 to 14. Formation and burst of short bubble were confirmed in these figures at both “Clean” and “Nose Roughness” conditions. Therefore, the adverse Reynolds number effect is never generated because of no

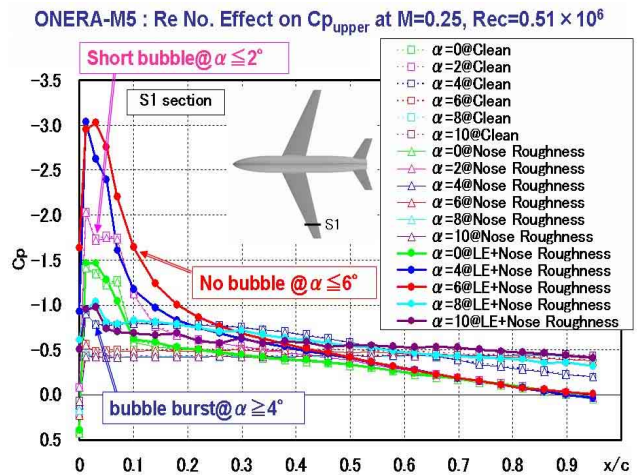


Fig. 12(a). Measured pressure distributions on the upper surface of outer wing at M=0.25 and Rec=0.51 million

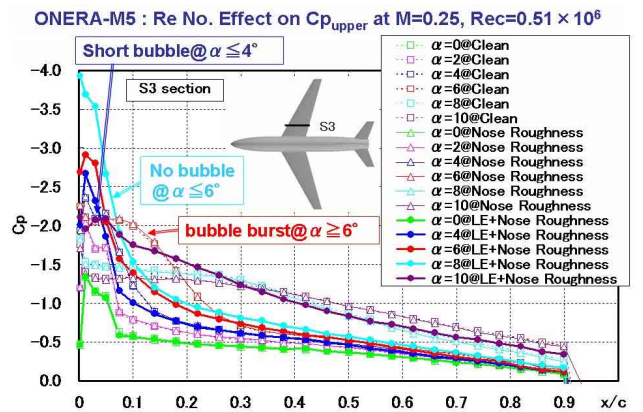


Fig. 12(b). Measured pressure distributions on the upper surface of inner wing at M=0.25 and Rec=0.51 million

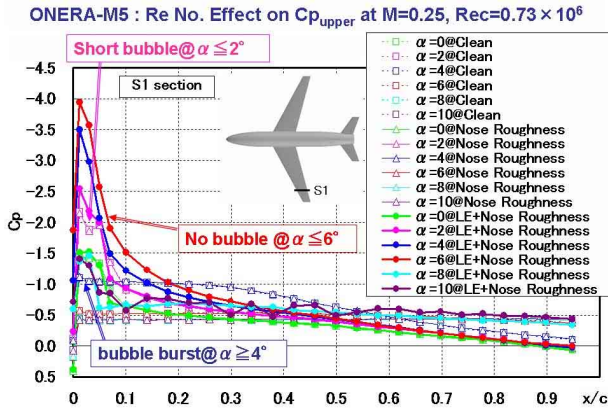


Fig. 13(a). Measured pressure distributions on the upper surface of outer wing at M=0.25 and Rec=0.73million

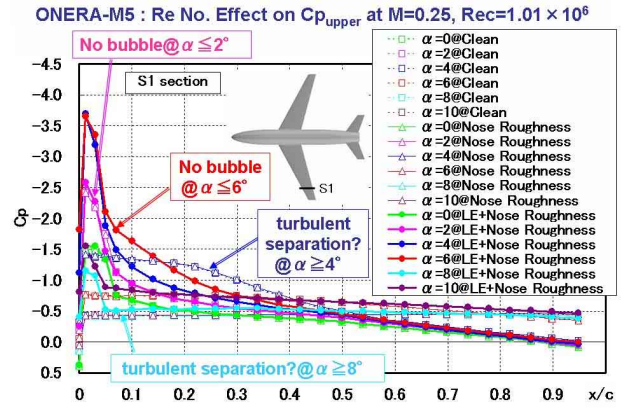


Fig. 14(a). Measured pressure distributions on the upper surface of outer wing at M=0.25 and Rec=1.01million

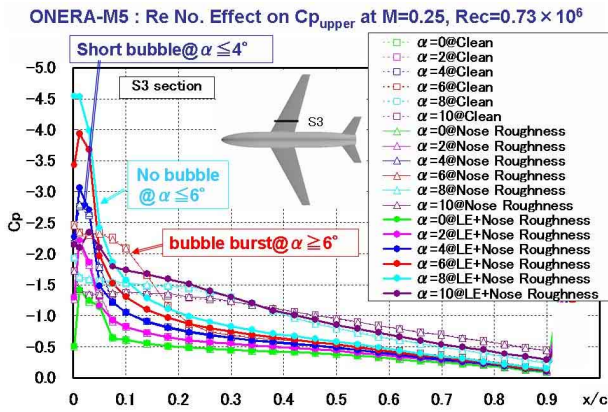


Fig. 13(b). Measured pressure distributions on the upper surface of inner wing at M=0.25 and Rec=0.73 million

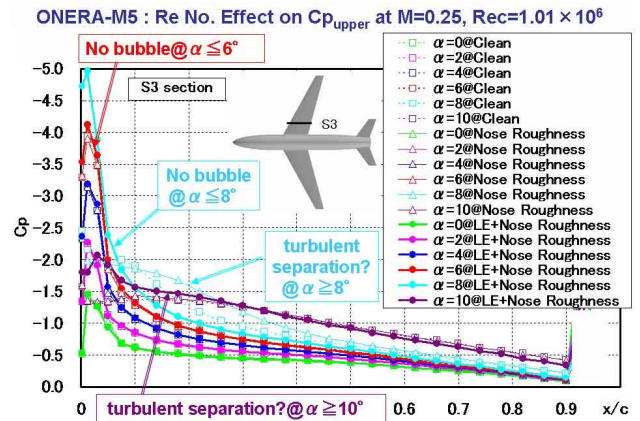


Fig. 14(b). Measured pressure distributions on the upper surface of inner wing at M=0.25 and Rec=1.01million

turbulent boundary layer near the attachment-line.

On the other hand, at the “LE+Nose Roughness” condition, the formation and burst of short bubble were not recognized clearly. And larger suction peak was observed at higher angle of attack. The “LE+Nose Roughness” condition produces meaningful transformation from the typical pressure distribution with short bubble to the different pressure distribution without any short bubble. Therefore, remarkable decrease of the lift due to its short bubble burst was suppressed by such transformation of the pressure distribution type. Also this is clearly demonstrated in Figure 15. This figure shows the measured total pressure of the Preston tube placed at 10% chordwise station on the right wing surface. The effect of the “LE+Nose Roughness” is reflected in suppressing the

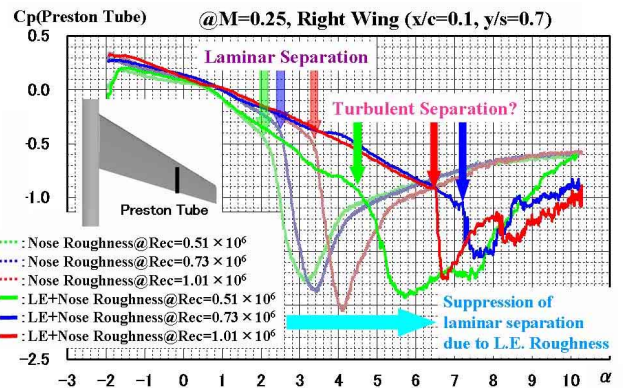


Fig. 15. Measured pressure of Preston tube at 10% chordwise location on the upper surface of outer wing at M=0.25

laminar separation.

3.2 CFD Analysis

From the test results mentioned above, we

can not deny any possibility of relaminarization near the leading-edge at the “LE+Nose Roughness” condition. To confirm that the “LE+Nose Roughness” condition completely leads to turbulent state on the wing surface, we tried to analyze the flowfield around the ONERA-M5 model using JAXA’s CFD(NS) code with all turbulent condition.

Figure 16 shows lift characteristics comparing with test results. Although the computed lift curve is slightly shifted in the direction of increasing angle of attack, lift slope is almost similar to the test result with the “LE+Nose Roughness” case. In the figure, a computed lift curve with an offset of the angle of attack, $\Delta\alpha=-0.5^\circ$ was also plotted as a reference. At least, we obtained very good agreement between the test result and the shifted computed result below $\alpha=6^\circ$. This implies that the “LE+Nose Roughness” condition makes boundary layer on the wing surface be in turbulent state clearly.

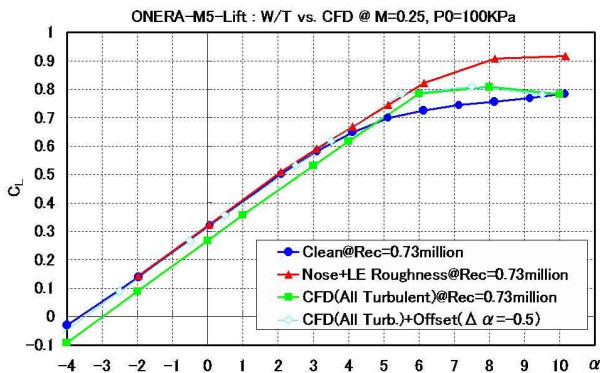


Fig. 16. Comparison of measured and computed lift characteristics at M=0.25

Figure 17 shows the comparison between measured pressure distributions and computed ones. We obtained very good agreement between the test result at the “LE+Nose Roughness” condition and CFD result with all turbulent condition at each spanwise station. Consequently, since the turbulent boundary layer on the wing surface did not induce the formation and burst of the short bubble, the maximum lift of the model was increased at higher angle of attack. And this means whole turbulent state on the wing surface is very

effective to increase the lift in suppressing the short bubble burst. However, it is completely different from the fact that full turbulent state from the leading-edge decreases its section lift which is a key mechanism of the adverse Reynolds number effect on lift characteristics.

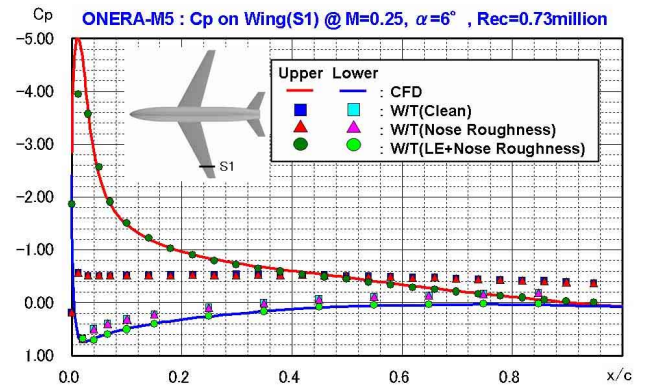


Fig. 17(a). Comparison of measure and computed pressure distributions on the upper surface of outer wing at M=0.25 and $\alpha=6^\circ$

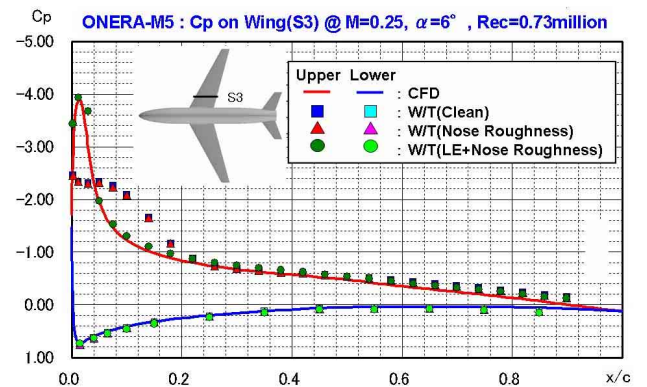


Fig. 17(b). Comparison of measure and computed pressure distributions on the upper surface of inner wing at M=0.25 and $\alpha=6^\circ$

Finally, we consider a hypothesis to explain this contradiction. The main points are as follows: the first point is that the adverse Reynolds number effect is supposed to be generated at relatively higher Reynolds number condition where any short bubble disappears. The second point is that the relaminarization is supposed to be induced in very narrow region near the suction peak point of the wing. We think that the wing section of the ONERA-M5 model has large potential of relaminarization

due to its strong acceleration near the leading edge even though boundary layer on the attachment-line is turbulent. And then, rapid transition just downstream the suction peak point is assumed to be generated without laminar separation, because its re-laminar state is not completely the same as usual laminar state. However, this hypothesis is just one candidate to explain present contradiction. In near future, we will investigate the validity of such hypothesis and also physical mechanism of high Reynolds number effect on the lift characteristics in detail.

4 Concluding Remarks

As for the transition characteristics of the ONERA-M5 model at transonic speed, we obtained useful experimental data and confirmed high correlation between transition measurement results and prediction results. As for the Reynolds number effect on the lift characteristics, the model has no possibility of the adverse effect in the test Reynolds number range, that is the normal Reynolds number effect, because the boundary layer on the wing surface is dominated by the formation and burst of the short bubble.

Acknowledgements

The authors would like to express special thanks to the staff of Wind Tunnel Technology Center of JAXA for their cooperative efforts to the preparation and wind tunnel operation with their ONERA-M5 model. And authors are also deeply indebted to Mr. Hiroaki Ishikawa of JAXA for his great efforts to conduct great number of CFD(NS) computations, and would like to acknowledge strong support for the test operation from Mitsubishi Heavy Industries , Ltd..

References

[1] Arnal D. Boundary Layer Transition : Prediction Based on Linear Theory, *AGARD FDP/VKI Special Course on Progress in Transition Modeling*, AGARD Report 793, 1993

- [2] Ueda, Y. Ishikawa H. and Yoshida K. Three Dimensional Boundary Layer Transition Analysis in Supersonic Flow Using A Navier-Stokes Code, ICAS 2004-2.8.2, 2004
- [3] Hardy B.C. Experimental Investigation of Attachment-line Transition in Low-Speed, High-Lift Wind Tunnel Testing, AGARD-CP-438, 2-1, 1989
- [4] Mach M.D. and McMasters J.H. High Reynolds Number Testing in Support of Transonic Airplane Development, AIAA-92-3982, 1992
- [5] Yoshida K. and Ogoshi H. Study for Reynolds Number Effect on C_{lmax} of 2-Dimensional airfoils, ICAS 96-3.1.2, 1996
- [6] Yoshida K. and Noguchi M. Adverse Reynolds number Effect on Maximum Lift of Two Dimensional Airfoils, ICAS 2000, Poster Session, ID295, 2000
- [7] Yoshida K. Ishida Y. Noguchi M. Ogoshi H. and Inagaki K. Experimental and Numerical Analysis of Laminar Flow Control at Mach 1.4, AIAA-99-3655, 1999
- [8] Takaki Y. Yamamoto K. Yamane T, Enomoto S. and Mukai J. The Development of the UPACS CFD Environment. In Viedenbaum A. Joe K. Amano H. Aiso H. editors, *High Performance Computing, 5th International Symposium, ISHPC 2003*, Tokyo-Odaiba, Japan, October 2003, Proceedings, volume 2858 of Lecture Notes in Computer Science, pages 307-319, Springer, 2003
- [9] Kaups K. and Cebeci T. Compressible Laminar Boundary Layer with Suction on Swept and Tapered Wings. *J. Aircraft* Vol.14, No.7, July, pp.661-667, 1977
- [10] Fujii, K. Sato M. Kanda H. Noguchi M. Mitsuo K. and Hosoe N. A Wind Tunnel Test on Transition Measurement Technique at Transonic Speed, *Proceedings of the 36th Fluid Dynamics Conference in Japan*, September 2004 (in Japanese)